Lattice disorder and oxygen migration pathways in pyrochlore and defect-fluorite oxides

Frederick P. Marlton[1], Zhaoming Zhang[2], Yuanpeng Zhang[3], Thomas E. Proffen[3], Chris D. Ling[1], Brendan J. Kennedy[1]

1. *School of Chemistry, The University of Sydney, Sydney, NSW 2006, Australia*
2. *Australian Nuclear Science and Technology Organisation, Lucas Heights, NSW 2234, Australia*
3. *Neutron Scattering Division, Oak Ridge National Laboratory, Oak Ridge, TN 37831, USA.*

Atomic-scale disorder plays an important role in the chemical and physical properties of oxide materials. Pyrochlore oxides, with general formula $A_2B_2O_7$, exhibit chemical structural flexibility, resulting in a diverse range of technological applications. The structure type adopted by $A^{III}{}_2B^{IV}{}_2O_7$ compounds is governed by the ratio of the ionic radii of the *A* (r_A) and *B* (r_B) cations. When r_A/r_B = 1.46 – 1.78, the structure is pyrochlore; while for r_A/r_B < 1.46 the structure is a disordered defect-fluorite. A recent study claimed the local structure of the defect-fluorite to be weberite-type[1], which we show is **not** the case.

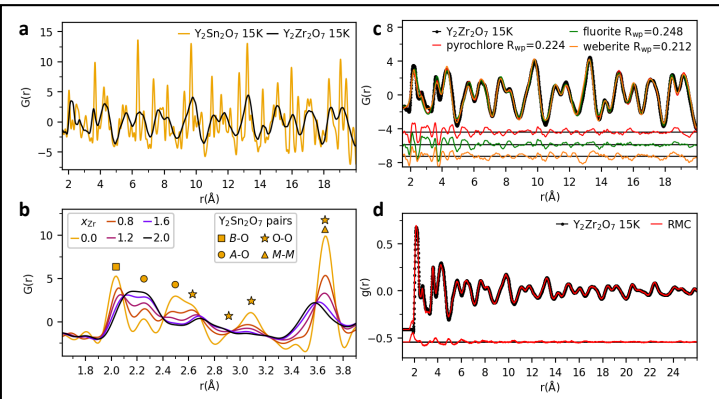

Neutron total scattering data and fitting at 15 K for samples in the $Y_2Sn_{2-x}Zr_xO_7$ series. a, PDF data of the $Y_2Sn_2O_7$ and $Y_2Zr_2O_7$ end-members for 1.6 ≤ r ≤ 20.0 Å, illustrating the difference in local disorder **b**, PDF data of all measured compositions for 1.6 ≤ r ≤ 3.9 Å illustrating the changes in local structure. Markers have been included to indicate peaks of the nearest-neighbor atom-atom pairs in the $Y_2Sn_2O_7$ pyrochlore structure. *M*–*M* refers to all possible cation-cation pairs. **c**, Small-box modelling fits to the $Y_2Zr_2O_7$ data with pyrochlore ($Fd\bar{3}m$), defect-fluorite ($Fm\bar{3}m$) and weberite (*Ccmm*) structural models and their difference curves offset below. **d**, Big-box modelling fit to the $Y_2Zr_2O_7$ data with difference curve offset below.

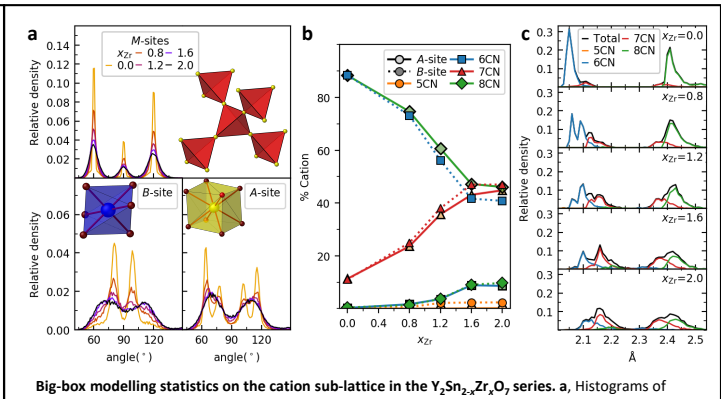

Big-box modelling statistics on the cation sub-lattice in the $Y_2Sn_{2-x}Zr_xO_7$ series. a, Histograms of various bond angles surrounding the cations, with insets showing the structural configurations. The top panel shows the nearest-neighbor angles between all cations (*M*). The bottom panels show the O–*M*–O bond angles surrounding the *B* (left) and *A* (right) cations. This shows the gradual increase in local disorder with Zr. **b**, Percentage of *A* and *B* site cations with coordination numbers between 5 and 8 as a function of Zr content, showing the changes in local coordination environments. **c**, Histograms of average *M*–O bond distances for each cation in $Y_2Sn_{2-x}Zr_xO_7$, color-coded by coordination number.

In the work reported here, we use low temperature neutron pair distribution function (PDF) to understand the evolution of local-scale structure in the $Y_2Sn_{2-x}Zr_xO_7$ system[2], which has its long-range average structure ranging from pyrochlore (*x* = 0) to defect-fluorite (*x* = 2). Data was measured at the NPDF diffractometer at Lujan Center, Los Alamos National Laboratory, USA. Using a combination of small- and big-box modelling, we found that the local structure of the defect-fluorite in the $Y_2Sn_{2-x}Zr_xO_7$ system is too complex to be modelled by the weberite structure. This also provide a quantitative picture of anion ordering that can be used to understand oxygen migration pathways, and hence design new and improved electrolytes for solid oxide fuel cells.

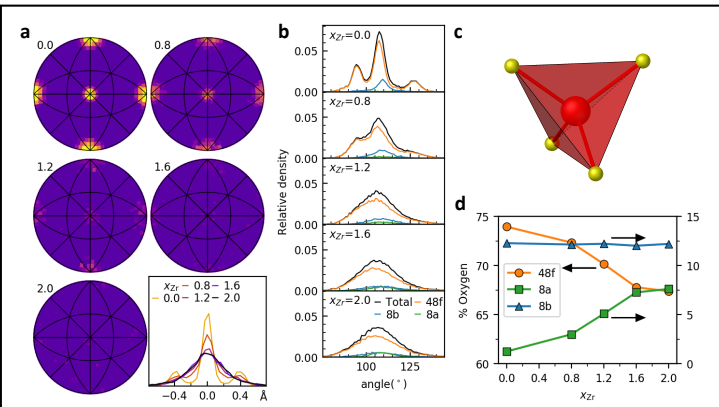

Big-box modelling statistics on the anion sub-lattice in the $Y_2Sn_{2-x}Zr_xO_7$ series. a, Stereographic projections and histograms of oxygen atomic displacements relative to an ordered fluorite structure illustrating the removal of locally ordered oxygen with Zr.. The stereographic projections are viewed down the [001] direction and the brightness corresponds to the density. Numbers on the top left corner of each stereograph correspond to the Zr (*x*) content. The histograms correspond to displacements along the x-axis only, with numbers in the legend corresponding to the Zr (*x*) content. In this representation, each of the stereographic projections is plotted on the same color scale. **b**, Histograms of *M*–O–*M* bond angles (*M* = cation) in all OM_4 tetrahedra (black) and individual oxygen sites (colored) for each of the $Y_2Sn_{2-x}Zr_xO_7$ compositions. **c**, OM_4 anion tetrahedral structure. **d**, Percentage of oxygen atoms in each of the three anion sites in the $Fd\bar{3}m$ structure as a function of Zr content. Arrows indicate which y-axis each line is plotted against. With Zr content, the oxygen is moving from the 48f to the 8a Wyckoff site.

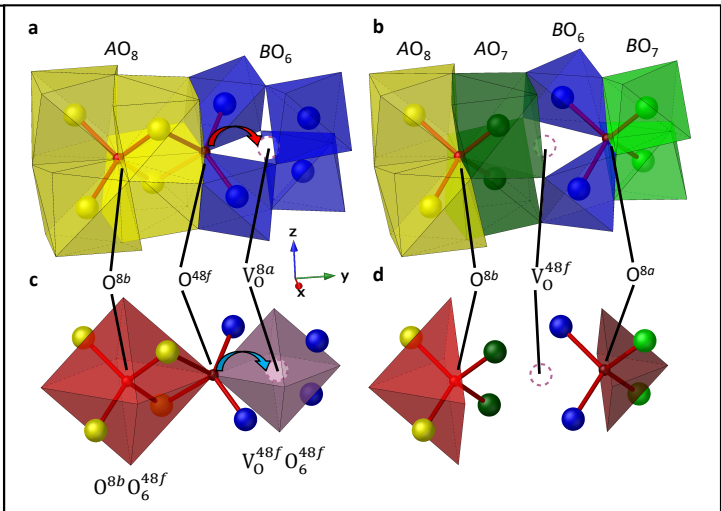

Illustration of oxygen migration associated with the transition from ordered pyrochlore (a,c) to defect-fluorite (b,d). Yellow and dark green spheres and polyhedra correspond to 8- and 7-coordinate *A* sites. Blue and light green spheres and polyhedra correspond to 6- and 7-coordinate *B* sites. The polyhedra in **a** and **b** represent the oxide ions coordinating those cations. The polyhedra in **c** and **d** represent interstitial non-bonding octahedra formed by the *48f* oxygens around the *8b* and *8a* sites, to illustrate the effects of oxygen migration on the anion sub-lattice.

Our results highlight the importance of collecting data at low temperatures, to minimize dynamic thermal disordering when studying the local structure of statically disordered solid-state materials.

[1]Shamblin, J., et al. (2016). Nature Materials **15**(5): 507-511.

[2]Zhang, Z., et al. (2013). The Journal of Physical Chemistry C **117**(50): 26740-26749.